Percolation on Strings and the Cover-up of the $c = 1$ Disaster

Geoffrey Harris

Dept. of Physics,
Syracuse University,
Syracuse, NY 13244, USA

gharris@npac.syr.edu

March 17, 1994

Abstract

We study percolation on the worldsheets of string theory for $c = 0, 1/2, 1$ and 2. For $c < 1$ we find that critical exponents measured from simulations agree quite well with the theoretical values. For $c = 1$ we show how log corrections determined from the exact solution reconcile numerical results with the KPZ predictions. We extend this analysis to the large c regime and estimate how finite-size effects will effectively raise the ground state energy, masking the presence of the tachyon for moderate values of $c > 1$. It thus appears likely that simulations for $c = 2, 3 \ldots$ on numerically accessible lattices will fail to even capture the qualitative behavior of the continuum limit.

1 Introduction

Within the last few years, the critical behavior of low–dimensional ($c \leq 1$) string theories has been understood in considerable detail. In particular, both analytic and numerical work has yielded a description of the intrinsic geometry of the worldsheet of these models [1, 2, 3, 4]. The worldsheet has been shown to be very spiky and branched; it can be characterized by a scaling distribution of embryonic universes [5, 6]. As c increases towards 1, embryonic universes of all sizes but with necks of the order of the cutoff proliferate and perhaps saturate the worldsheet.

A direct determination of properties of the intrinsic geometry of string theories constructed from $c > 1$ matter has proven much more difficult. There are many theoretical indications that the worldsheet degenerates into polymer-like configurations above $c = 1$. Though the $c < 1$ surfaces are quite spiky, they still appear to retain some of the character of two dimensional surfaces; this perhaps is no longer true for $c > 1$. For at $c = 1$ the dressed identity operator (coupled to the cosmological constant) becomes tachyonic. Above $c = 1$, this operator should then spawn states which are non-local in the worldsheet metric that effectively tear the worldsheet apart [7, 8]. Related computations in Liouville theory indicate that a sort of Kosterlitz Thouless transition is anticipated at $c = 1$, in which vortex configurations of the Liouville field become unbound [9]. Unfortunately though, this picture has not been verified via an exact calculation for

$c > 1$; the appropriate matrix models have not been amenable to exact solution (though see [10] and [11]) and Liouville theory yields complex exponents in this regime. We would therefore like to detect, through Monte Carlo simulations, some characteristic of the geometry of worldsheets that distinguishes $c \leq 1$ from $c > 1$ and signals the onset of the tachyon.

In fact, numerical work has not provided any evidence of a dramatic change in the internal geometry of the worldsheet as c passes 1. Simulations, albeit on modest-sized lattices, only have shown convincing evidence of branched-polymer structure on the worldsheet for $c > 10 - 12$. Recently, there has been much work on simulations of multiple Potts models coupled to gravity [12, 13, 14]; the systems studied generally have small values of c both greater and less than 1. In these studies, the internal geometry was characterized by measuring the distribution of discrete curvature, or more precisely, the distribution of ring lengths on ϕ^3 graphs dual to triangulations. These measurements indicated that no dramatic change in these curvature distributions occurs as c is increased above 1. Interpreting these results rigorously is difficult, though, since it is not clear how to identify these curvature distributions with continuum (universal) correlation functions.

To search for a transition to branched polymers, Ambjørn et al. [12] also simulated Ising models on typical fixed random triangulations sampled from the set of worldsheets characteristic of gravity coupled to matter of central charge c. Each triangulation was generated during a simulation of a multiple Potts or Gaussian models coupled to gravity; the Ising model was then simulated on each of these particular triangulations. These authors showed that the Ising model on a branched polymer will not undergo a phase transition. Only when c reached or exceeded 12 did they find that no finite-temperature Ising transition was evident on the surfaces extracted from their simulations.

For fairly low central charge, the coupling between matter and gravity, as inferred from the above numerical work, *appears* to be fairly weak, perhaps too weak to drive the worldsheet into a branched polymer phase [12]. It has thus been suggested that worldsheets of gravity coupled to matter with $c > 1$ but less than about 10 might lie in some sort of intermediate phase and not undergo a transition to branched polymers for c above 10 or so [15, 12]. Such a scenario is quite intriguing, especially since the existence of such a phase does not seem to be anticipated by Liouville theory.

To reveal the character of the critical geometry of string worldsheets, we shall examine site percolation on dynamical triangulations coupled to matter. The distribution of percolation clusters should serve as a sensitive probe of the branched structure of the worldsheet, distinguishing $c \leq 1$ from a branched polymer phase. Essentially, embryonic universes act as traps that prevent percolation

clusters from growing, while regions of high connectivity will enhance the span of percolating clusters. We also indicate how the critical behavior of percolating clusters on worldsheets of $c < 1$ matter coupled to gravity can be determined from Liouville theory. The quality of the results of numerical simulations of two-dimensional gravity has often been called into question, with the suspicion that the lattices used were often too small to even qualitatively reflect continuum behavior. We shall see however that we can reproduce on lattices of several thousand nodes, with quite good precision (of order 1%), the theoretical predictions of these percolation exponents for $c < 1$. At $c = 1$, matrix model solutions and Liouville theory [16] predict a more complicated logarithmic dependence of correlation functions on the cosmological constant. We also find that our results are consistent with the functional dependence predicted by matrix models along with the exponents of Liouville theory. Our data shows only an apparent weak coupling of $c = 1$ matter to gravity, but this is misleading. The logarithmic scaling of the matrix model implies that effectively $c = 1$ matter only has a small effect on the percolative structure of the lattice for small lattice sizes. For larger lattices however, the matrix model solutions predict that the influence of the matter coupling to gravity should gradually become more pronounced.

We also will demonstrate that percolation on non-interacting branched polymers does not undergo a transition for $p < 1$. We shall then find evidence suggesting that for $c = 2$, the critical behavior of percolating clusters (or indeed perhaps the lack of criticality) may be qualitatively different from that of $c < 1$. The $c = 2$ observations, which need to be interpreted with great care, *at first glance* appear to be indicative of a breakdown of the behavior that characterizes percolation on surfaces.

In illuminating the above results, we shall argue that for c somewhat greater than one, the finite size of the lattice will largely mask the theoretically anticipated degeneration of the worldsheet. The infrared cutoff should induce a large shift in the tachyonic energy, preventing the unrestrained proliferation of tachyons on not too large lattices. We can, in fact, estimate the magnitude of this effect. With this in mind, we then argue that for c somewhat greater than 1, we are most likely measuring finite-size artifacts; yet the presence and qualitative nature of these effects can be understood in the context of string theory.

A delicate analysis of percolation on dynamically triangulated lattices is possible largely due to a curious but elementary graphical property of triangulations: they are self-matching. This constrains the value of the percolation threshold to be 1/2, with a few caveats. We shall explain this further in Section 3.

In a companion paper [17], an analysis of the critical properties of the

two-species Ising model coupled to two-dimensional gravity appears. As in this paper, it is essential to incorporate logarithmic corrections to scaling to compare numerical results with theory. Percolation is also simulated on random lattices coupled to two Ising species, yielding results consistent with those presented here.

The plan of this paper is as follows. We begin by reviewing basic facts about percolation and discuss how the KPZ [18] equation predicts the behavior of percolating clusters on $c < 1$ dynamical lattices. We then explain the theoretical predictions for $c = 1$ and also analyze the behavior of percolation on branched polymers. A discussion of the constraint $p_c = 1/2$ follows. We then describe the numerical techniques we have used, including an analysis of auto-correlations. We next present the results of our simulations (for $c = 0, 1/2, 1$ and 2) and then give our conclusions.

2 Theoretical Predictions

We shall present the results of site percolation on random lattices sampled from simulations of quantum gravity coupled to matter. Site percolation describes the following process: we randomly color sites 'black' on a lattice with probability p. Adjacent black sites are then connected together to form clusters. We shall generally be interested in features of the distribution $n(s)$ of these clusters as a function of the number of constituent sites s. Typically, we will measure the mean cluster size, denoted by $\mathcal{S}$. If one randomly chooses a black point on the lattice, then on average it will belong to a cluster of size s. Explicitly, $\mathcal{S} = \langle s^2 \rangle / \langle s \rangle$, in which averages are taken over the distribution $n(s)$. If a percolation transition occurs at some value $p = p_c$, then in the infinite volume limit, $\mathcal{S}$ remains finite for $p < p_c$ but diverges (it is proportional to the number of lattice sites N) for $p > p_c$ due to the presence of an infinite cluster. The mean size can also be written as the integral of the pair-connectedness function

$$\mathcal{S}_N = \frac{1}{N} \sum_{i,j=1}^{N} \langle \delta_{\mathcal{C}_i, \mathcal{C}_j} \rangle; \tag{1}$$

the quantity within the bra-ket is 1 when i and j lie in the same cluster and 0 otherwise.

One can also consider bond percolation, in which bonds of the lattice are randomly colored black with probability p and clusters are then constructed from sites connected by black bonds. Bond percolation is generically in the same universality class as site percolation. A bond percolation problem on a lattice L, for instance, can be mapped exactly to site percolation on the covering lattice

of L (as defined in reference ([19])). The properties of bond percolation clusters can be derived by appropriate averaging with the partition function

$$Z = \sum_{colorings} p^b (1-p)^{N_b - b} q^{N_c} \tag{2}$$

with $q \to 1$; b equals the number of black bonds that constitute N_c clusters in a lattice with N_b total bonds. In fact, the partition function of the q-state Potts model on this lattice can be recast as (2); thus percolation is a non-interacting limit of these theories. The $q \to 1$ Potts model coupled to gravity has been studied analytically as a matrix model by Kazakov [20]. This mapping provides an interpretation of typical percolative properties in the language of spin models. For instance, the relation (1) is analogous to the equivalence of the susceptibility ($\mathcal{S}$) and the integral of the spin-spin correlation function. The scaling behavior of this correlation function can then be computed exactly in 2 dimensions via a mapping of the Potts model to the Coulomb gas [21]. The result is

$$\langle \delta_{\mathcal{C}_i, \mathcal{C}_j} \rangle \sim |\vec{r}_i - \vec{r}_j|^{-2(\Delta^o_{\sigma, q=1} + \bar{\Delta}^o_{\sigma, q=1})}, \tag{3}$$

with $\Delta^o_{\sigma, q=1} = \bar{\Delta}^o_{\sigma, q=1} = 5/96$ [1].

The random surfaces which we shall examine are triangulations of two-dimensional geometries. The discretization we use consists of a sum over all possible triangulations of N vertices, excluding degenerate triangles [2], with weights determined by the partition function

$$Z_N = \sum_{T \in \mathcal{T}_N} \rho(T) \exp(-\mathcal{H}_{matter}); \tag{4}$$

$\mathcal{H}_{matter}$ is the Hamiltonian for Ising or Gaussian fields and $\rho(T)$ is the measure in the space of triangulations $\mathcal{T}_N$ of N vertices. Most of the relevant theoretical calculations are performed in the grand-canonical ensemble, with the partition function

$$Z(\mu) = \sum_{N=1}^{\infty} Z_N \exp(-\mu N) \tag{5}$$

dependent on μ, the cosmological constant. The integrated pair-connectedness correlation function in the grand-canonical ensemble then satisfies

$$\left(\sum_{i,j} \delta_{\mathcal{C}_i, \mathcal{C}_j} \right)(\mu) Z(\mu) = \sum_{N=1}^{\infty} N \mathcal{S}_N Z_N \exp(-\mu N). \tag{6}$$

---

[1] The weight $\Delta^o_{\sigma, q=1}$ is *not* identified with a local operator in percolation theory; it just determines the scaling behavior of a certain class of correlation functions.

[2] i.e. those with loops of length 1 or 2 or vertices with fewer than 3 neighbors.

We will thus simulate the tensor product of the $q = 1$ Potts model with the matter theory coupled to gravity. Only, since percolation is not dynamical, it does not generate any back-reaction on the gravity or the matter. Using standard arguments [3], ([22]) one can express the scaling behavior of the integrated pair-connectedness correlation function of percolation coupled to gravity via the KPZ formula ([18]). The weight $\Delta_{\sigma,q=1}^\circ = \tilde{\Delta}_{\sigma,q=1}^\circ = 5/96$ is dressed by gravity in a theory of central charge $c = c_{matter} \leq 1$ ($c_{percolation} = 0$) so that

$$\Delta_{\sigma,q=1} - \frac{5}{96} = \left(1 + \frac{1}{12}\sqrt{1-c}(\sqrt{1-c} - \sqrt{25-c})\right)\Delta_{\sigma,q=1}(1 - \Delta_{\sigma,q=1}). \quad (7)$$

This dressed weight determines the scaling of the integrated pair-connectedness function with μ on surfaces of genus h:

$$\left\langle \sum_{i,j} \delta_{c_i,c_j}\right\rangle(\mu)Z(\mu) \sim (\mu - \mu_c)^{2(-1+\Delta_{\sigma,q=1})+(2-\gamma_s)(1-h)} \quad (8)$$

(the -1 before the dressed weight accounts for the integrations of i and j over the surface) with

$$\gamma_s = \frac{1}{12}\left(c - 1 - \sqrt{(25-c)(1-c)}\right). \quad (9)$$

Then the relation (6) and

$$Z_N \sim N^{-1+(\gamma_s-2)(1-h)} \quad (10)$$

yield the finite-size scaling relation

$$S_N \sim N^{1-2\Delta_{\sigma,q=1}}; \quad (11)$$

this is the scaling law that we shall verify numerically. As more generally in spin models, the above exponent is referred to as $\gamma/\nu d_H$. The mean cluster size satisfies $S \sim (p - p_c)^{-\gamma}$, the correlation length (governed by the decay of the pair-connectedness function) $\xi \sim (p - p_c)^{-\nu}$ and d_H is the intrinsic Hausdorff dimension of the random surface being considered. We also shall measure the fractal dimension of the largest cluster at p_c; the average maximal size cluster of each configuration $\mathcal{M}$ scales as

$$\mathcal{M} \sim N^{\frac{d_f}{d_H}}. \quad (12)$$

Standard scaling arguments [24] relate $\gamma/\nu d_H = 2d_f/d_H - 1$.

[3] applied to the integrated two point function rather than the one point function as usually presented

2.1 $c = 1$

The scaling relations become more complicated for $c = 1$. The analytic solutions of the $c = 1$ matrix models [23] and a careful analysis of Liouville theory show that correlation functions no longer scale simply as powers of the cosmological constant μ. Instead, the appropriate scaling variable is η which satisfies [4]

$$\mu = -\eta\ln(\eta) + c_1\eta + \cdots \quad (13)$$

in the limit of small η; c_1 is a constant that we do not specify. The analytic solution employs a modified Gaussian propagator on phi-cubed lattices and is thus not based on the same discretization that we use in our simulations. We shall assume that the asymptotic scaling relation also holds for the model we simulate; we will not presume universality for the subleading coefficient c_1. We therefore conjecture that the scaling relation (8) should be modified so that

$$\left\langle \sum_{i,j}\delta_{c_i,c_j}\right\rangle(\mu)Z(\mu) \sim \eta(\mu)^{2(-1+\Delta_{\sigma,q=1})+(2-\gamma_s)(1-h)}. \quad (14)$$

Our simulations will be done on worldsheets of toroidal topology ($h = 1$) for which $Z(\mu) \sim \ln(\eta)$ for $c = 1$. To extract the asymptotic scaling behavior of S_N, we invert the relation between η and μ order by order in $1/\ln\mu$ and $\ln(-\ln(\mu))/\ln(\mu)$ to obtain

$$\eta = -\frac{\mu}{\ln\mu}\left(1 + \frac{\ln(-\ln\mu)}{\ln\mu} + \left(\frac{\ln(-\ln\mu)}{\ln\mu}\right)^2 - \frac{\ln(-\ln\mu)}{(\ln\mu)^2} + \cdots\right). \quad (15)$$

We then expand the inverse Laplace transform of (14) to obtain

$$NS_N Z_N \sim \frac{1}{N(N\ln N)^\omega}\left(1 - \frac{\ln\ln N}{\ln N} + \left(\frac{\ln\ln N}{\ln N}\right)^2 - \frac{\ln\ln N}{(\ln N)^2} + \cdots\right)^\omega \times \left(1 + \frac{\omega\Psi(-\omega)}{\ln N} - \omega\Psi(-\omega)\frac{\ln\ln N}{(\ln N)^2} + \cdots\right); \quad (16)$$

$\omega = 2(-1+\Delta_{\sigma,q=1}) = -\gamma/\nu d_H - 1$ and Ψ is the digamma function. The scaling behavior of NZ_N is obtained by inverse Laplace transforming $\partial Z(\eta(\mu))/\partial\mu$:

$$Z_N \sim \frac{1}{N}(1 + \frac{1}{\ln N} - \frac{\ln\ln N}{(\ln N)^2} + \cdots). \quad (17)$$

In addition to the higher order terms that we have dropped from the inversion, there are additional corrections to the above formulae. The corrections to the

[4] Without loss of generality, we set $\mu_c = 0$.

logarithmic renormalization of μ which depend on c_1 in (13) should lead to contributions to (16) and (17) that are competitive with the smallest corrections we have shown. We neglect the usual corrections to scaling that are suppressed by (non-integer) powers of $1/N$. To compare this finite-size scaling form with our data, we shall present a plot of $\ln(S_{2N}/S_N)/\ln 2$ computed from (16) and (17). The leading logarithmic contributions that we have derived above will turn out to be very significant [5].

2.2 $c \gg 1$

We are particularly interested in using percolation to uncover the character of the internal geometry of surfaces for $c > 1$. In this regard, we discuss the behavior that we would anticipate in the large c limit. Ambjørn, Durhuus, Fröhlich and Orland [26] have argued that in the large c (d) limit, the string path integral (with appropriate measure) should be dominated by surfaces that form a branched-polymer like structure. To show this, they essentially perform a saddle-point evaluation of the string path integral

$$Z = \sum_{T \in \tilde{\mathcal{T}}_n} (\prod_i q_i)^{d/2+\alpha} \int \prod_{i,\mu} dX_i^\mu \exp\left(-\sum_{i,j} C_{ij} \sum_{\mu=1}^d (X_i^\mu - X_j^\mu)^2\right), \quad (18)$$

with the integration over the center of mass of $\vec{X}$ implicitly omitted. $\tilde{\mathcal{T}}_n$ represents the space of triangulations that do not contain loops of unit length or vertices of order less than 3. As usual, C_{ij} is the adjacency matrix of the triangulation T. For $i \neq j$, it equals the number of links connecting i and j; $C_{ii} = -q_i$; q_i is the coordination number of site i, equal to the number of links emanating from i. We can integrate out the Gaussian fields, obtaining $(\det' C_{ij})^{-d/2}$ (with the zero-mode omitted). It can be shown [26] that this determinant is minimized by surfaces consisting of tetrahedra glued together along a common pair of vertices. [6]. To perform the gluing, the link connecting these vertices within each tetrahedron is slit into two edges; each edge is then glued to a slitted edge of the adjacent tetrahedron. This process creates loops of length 2 which are allowed in $\tilde{\mathcal{T}}_n$, these are excluded from the set of triangulations $\mathcal{T}_n$ that we consider in our simulations. It has been shown that in $d = 0$ and -2, the critical properties are independent of whether loops of length 2 are included. Let us assume, as in reference ([26]) that this is also true in the large d limit, since the configurations that dominate the saddle point in the space $\mathcal{T}_n$ are quite

---

[5] The essential role of logarithmic corrections in interpreting numerical measurements of γ_s at $c = 1$ has been previously discussed in references [25, 5].

[6] This does not rule out the possibility of other saddle point solutions, though.
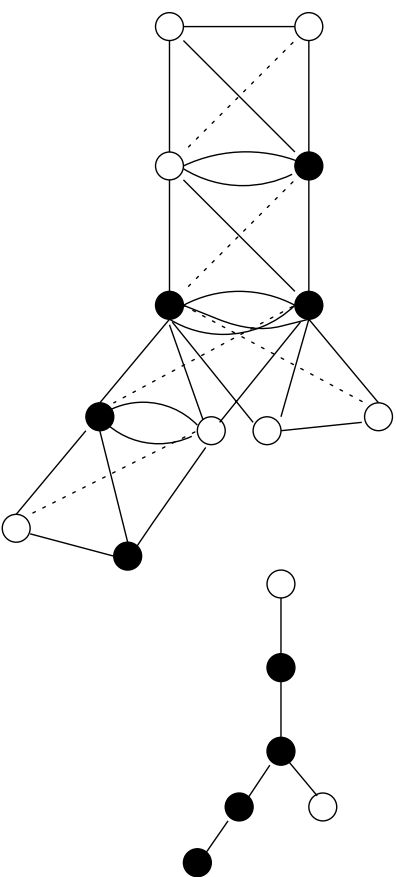
Figure 1: A sample triangulated surface built from linked tetrahedra, with vertices colored as in percolation. The arcs represent slitted edges. To the right, the associated branched polymer appears; each tetrahedron corresponds to a polymer link.

complicated and not amenable to the following simple analysis. We shall then analyze a class of triangulations discussed by Ambjørn et al. [12] that includes these saddle point solutions; this class is formed by linearly joining the linked tetrahedra that minimize the determinant. A typical triangulation is depicted in figure 1.

We first show that the percolation problem on this class of triangulations can be mapped to a percolation problem on the model of branched polymers considered by Ambjørn et al.. Each tetrahedron will correspond to a bond in a branched polymer. We identify an internal polymer vertex with a pair of sites connected by a slitted edge on the original triangulation. Vertices on the boundary of the polymer are associated with pairs of sites that lie adjacent at dead-ends of the triangulation. Now, if either of the two sites along a slit edge are colored black, then the percolation cluster to which they belong must include any of the black sites in adjacent tetrahedra. If an infinite percolation cluster is to wind through the lattice, its extent depends only on whether or not at least one of two sites on the original triangulation, associated with a polymer vertex, is black. Therefore, we identify black-black, black-white and white-black pairs of sites with a black polymer vertex; a white-white pair is mapped to a white polymer vertex. If we color sites on the triangulation with probability p, then at least one of a pair of sites is black with probability $p(p^*) = 1 - (1 - p^*)^2$. Thus if the percolation threshold on the original lattice is p^*, then the associated branched polymer will undergo a transition at $p(p^*)$.

We now show that these branched polymers (in their critical limit) do not admit a percolation transition for $p < 1$. They are described by the partition function [26]

$$Z = \sum_N \sum_{t \in t_N} \langle \prod_i w(q_i) \rangle \exp(-\mu N),$$
(19)

in which t_N represents the set of trees (graphs with no loops) of N vertices and each vertex with coordination number q_i is given a weight $w(q_i) = \prod_i (q_i)^\alpha$ (since the determinant of the adjacency matrix on these surfaces just effectively shifts the exponent in the measure).

The analysis of percolation on these polymers proceeds as in the case of the Bethe lattice [24]. First, we randomly select a site i on the lattice and a branch that emanates from it. Let T denote the mean number of sites in this branch that belong to the same cluster as i. If the neighbor j to site i in this branch has coordination number q_j then

$$T = p + p\langle q_j - 1 \rangle T;$$
(20)

the first contribution p is the probability that site i is black and in a cluster; if site j is black (with probability p) then each of its $q_j - 1$ subbranches contributes on average T sites. Therefore, $T = p/(1 - \langle q - 1 \rangle p)$. If we then randomly select a black site on the branched polymer, we see that on average it is part of a cluster of size

$$S = 1 + \langle q \rangle T = 1 + \frac{\langle q \rangle p}{(1 - \langle q - 1 \rangle p)},$$
(21)

where S is the mean cluster size. Hence percolation will occur on these trees as long as the density of dead ends ($q = 1$ vertices) is not large enough to reduce $\langle q \rangle$ below 2 and trap all percolating clusters. If $\langle q \rangle > 2$, then the mean cluster size behaves as if we were just considering a Bethe lattice.

Now we shall compute the mean coordination number in the critical limit for this model of non-interacting branched polymers. First, note that a polymer vertex of coordination number q is associated with two sites of the original triangulated surface with coordination number $3q$. If this surface is of infinite size and of finite genus, then simply $\langle 3q \rangle = 6$. One can also show in a slightly more painstaking fashion that this condition holds in the grand-canonical ensemble by analyzing the solution of the Schwinger-Dyson equations for Z analyzed by Ambjørn et al. [12]. The equations are written down for 'rooted' branch polymers, which emanate from a marked point with coordination number 1, they are represented graphically in figure 2. Z obeys

$$Z = \exp(-\mu)(1 + f(Z)); \quad f(Z) = \sum_{i=2}^\infty w(i) Z^{i-1}.$$
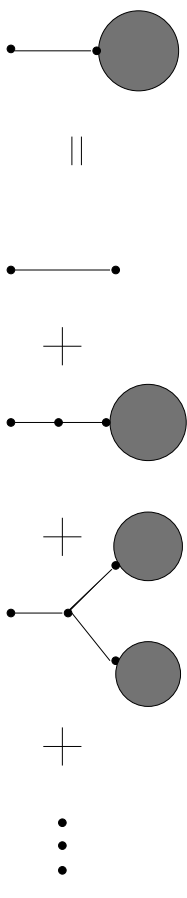(22)

Figure 2: The Schwinger-Dyson equations for the partition function of a rooted branched polymer.

Criticality occurs at $\mu = \mu_c$ such that $\partial Z/\partial \mu|_{\mu_c} \to \infty$ providing that f is convergent in $[0, Z(\mu_c)] \equiv Z_c]$; this criterion is satisfied for the measures that we will consider. $Z(\mu)$ will then have a leading singularity of the form $\sim (\mu - \mu_c)^{1/2}$. The mean coordination number (minus 1) equals

$$\langle q - 1 \rangle = \frac{\sum_{i>1}^\infty (i - 1) w(i) Z^i}{-\partial Z/\partial \mu}.$$
(23)

By differentiating the Schwinger-Dyson equation with respect to $w(i)$ and μ and substituting in above, we find that simply $\langle q - 1 \rangle = f'(Z) \exp(-\mu)$ which equals $1 - 1/\langle A \rangle$. $\langle A \rangle$ is the mean surface area which diverges at $\mu = \mu_c$. Therefore $S(\mu)$ (21) is non-singular for $\mu \geq \mu_c$ and $p < 1$. Thus criticality drives the percolation threshold p_c to 1. The partition function for the q-state Potts model on a branched polymer can also be analyzed in the limit $q \to 1$ (this was done for the Ising model in ([12])). From this one can obtain an exact formula for the number of clusters per unit area, which turns out to just depend linearly on p.

We close this section by reiterating that the equivalence of the behavior of percolation clusters on branched polymers (which we have analyzed) and on worldsheets in the large d limit relies on unproven assumptions. It is not perhaps so obvious that percolation on the saddle points in the space $\mathcal{T}_n$ will behave as on the saddle points of $\tilde{\mathcal{T}}_n$, which we may not even have completely characterized. Thus, these large d results should be interpreted with appropriate caution. The preceding arguments do, in any case, illustrate the behavior of percolation on a class of triangulations which form tree-like structures.

3 $p_c = .5$

We now turn to an examination of how the geometry of the lattice constrains the value of the percolation threshold. Consider the function $K(p) = N_c/N$, the number of clusters per unit area of the lattice. Sykes and Essam demonstrated

[27] that on any planar triangulated multiply-connected lattice,

$$K(p) = K(1-p) + 2p(p - \frac{1}{2})(p-1).$$ (24)

This relation is exact for finite N for planar lattices; for lattices with the topology of the torus, it is obeyed up to corrections of order $1/N$. The derivation of (24) is based on an application of Euler's theorem to the two subgraphs consisting of the set of all black (white) clusters. The $1/N$ corrections just arise from the genus term in Euler's equation for subgraphs embedded on surfaces of higher topology. The key element of the proof of (24) is the following simple fact: on any triangulation, each face consists of vertices which are *all* connected to each other.

The identity (24) is analogous to the duality relation for the free energy of the 2−d Ising model, though in this case the geometrical notion of lattice duality is quite different. We briefly digress to discuss this now. Consider a lattice $\mathcal{L}$ and select a set of faces $\mathcal{F}$. We then close-pack all faces $\mathcal{F}$; close-packing consists of linking all vertices on a face together. This yields a new graph $\hat{\mathcal{L}}$. Let $\mathcal{L}^*$ then be the lattice constructed by close-packing all faces in $\hat{\mathcal{L}}$ that are not in $\mathcal{F}$. Then (24) is a special case of the identity

$$K_{\mathcal{L}}(p) = K_{\mathcal{L}^*}(1-p) + \phi(p)$$ (25)

where ϕ is referred to as the matching polynomial. $\mathcal{L}$ and $\mathcal{L}^*$ are matching lattices; any triangulated lattice is self-matching.

The analogy with Ising duality has a bit more content, since if there is a transition at $p = p_c$, $K(p) \sim (p - p_c)^{2-\alpha}$. In the mapping of percolation to the q-state Potts model, α is the exponent that describes the singular behavior of the free energy (which obeys the Ising duality relation) and the specific heat. Thus, we can compute α for percolation coupled to $c \le 1$ gravity with the KPZ formula as in (7), substituting the weight of the energy operator ($\Delta_\epsilon^g = 5/8$) in the $q \to 1$ limit of the Potts model for the spin operator weight of $5/96$. Then assuming the standard hyperscaling relation, one finds that the dressed weight of the energy operator Δ_ϵ equals $(1 - \alpha)/(2 - \alpha)$. For percolation with no matter ($c = 0$), the form of $K(p)$ has been computed by Kazakov [20] by analyzing matrix model saddle point equations; $\alpha = -2$ and $K(p)$ also has logarithmic contributions to scaling. From the KPZ formula, we see that the exponent α then decreases with c, reaching an irrational value of $-(2\sqrt{10}+2)/3 \sim -2.77$ at $c = 1$.

Thus for $0 \le c \le 1$, $K(p)$ is always non-analytic at its critical point, and perforce by (24), $p_c = 1/2$. If the surfaces admit a percolation transition for $c > 1$ with a value of α that varies continuously with c, then p_c must still equal

1/2. If we discover that a transition no longer occurs near $p_c = 1/2$, then we can conclude that either that there is no percolation transition for $0 < p < 1$ (as for branched polymers) or possibly that a sort of mean-field percolation transition occurs. In the former case, two types of lattice behavior could occur. The first possibility would be a collapsed lattice in which virtually all vertices are connected to each other; such a lattice would have a finite probability of containing an infinite cluster for all $p > 0$. On the other hand, if the average connectivity were sufficiently low (as for the finite-genus surfaces constructed from gluing tetrahedra, discussed in the previous section), then no infinite clusters would occur for all $p < 1$ [7]. A 'mean-field' transition explicitly refers a transition in which α is constant and integral over a range of central charge. For instance, in flat space, the mean field solution for percolation (above $d = 6$) yields $\alpha = -1$; such a solution would describe trees with sufficiently high mean connectivity [8]. It is not so clear that one can construct a finite genus surface surface in the universality class of the Bethe lattice with $p < 1$; perhaps the mean-field scenario is also not allowed for $1/2 < p < 1$. In any case, both the mean-field and no-transition scenarios do seem to be characteristic of percolation on trees rather than surfaces; they should signify a qualitative change in the geometry of the worldsheet.

With this background, we now summarize our plan of attack. We will simulate percolation on $c \le 1$ worldsheets, checking that indeed $p_c = 1/2$ and verifying theoretical predictions for critical behavior. Assuming $p_c = 1/2$ will allow us to measure the exponents much more precisely than would usually be the case. For generically a slight mismeasurement in the critical temperature will induce a significant error in the finite-size scaling determination of critical exponents. Then to look for a degeneration of the worldsheet, we will attempt to determine if p_c is no longer near $1/2$ for $c > 1$.

4 The Simulation

We now provide a discussion of details of our simulation and analysis. Our simulations were performed on dynamically triangulated random surfaces (DTRS), using the standard flip algorithm [29] to update the adjacency matrix C_{ij}. The flip algorithm rejected updates that led to triangulations with loops of length 1 or 2 or vertices with coordination number less than 3. We examined DTRS with

---

[7] An example of an extremely branched triangulated lattice with $p_c = 1$ also is given in reference [28].

[8] A somewhat pathological example of a triangulated surface in this universality class with $p_c < 1$ consists of a lattice of connected tetrahedra with infinite genus (with $\langle q \rangle > 6$ and $p_c = 3/(\langle q \rangle - 3)$) described by the construction in the previous section. The identity (24) is no longer true for infinite genus surfaces, however.

no embedding coordinates as well as with Ising spins or Gaussian fields attached to the vertices (with interactions along the links).

Our action for the Ising model was $S = \beta_c \sum_{\langle ij \rangle} \sigma_i \sigma_j$. We chose a measure independent of q_i, as in the matrix model formulation. The Ising spins were updated using the Swendsen-Wang cluster algorithm[30]. Each update consisted of $3N$ attempted flips of randomly chosen links followed by a Swendsen-Wang update of the entire lattice. The critical temperature for Ising spins on lattices dual to our triangulations was computed analytically in [31], so by the standard Ising duality we can determine that $\beta_c = (1/2) \ln(131/85) \sim .216273$. This particular discretization of the Ising model has been studied in [32, 17].

For $c = 1$ and 2 we used a standard Metropolis algorithm, in which the Gaussian fields were updated via random shifts from a flat distribution. In the Gaussian case, $3N$ randomly chosen flips were performed and then $3N$ randomly chosen X coordinates were updated. We used the standard Gaussian action with the conformal measure, which corresponds to the choice $\alpha = 0$ in (18). We also simulated the $d = 1$ Gaussian model with the choice $\alpha = -1/2$ and found that the critical behavior (as determined from the calculation of finite-size scaling exponents) was identical, within our statistics, to that measured for $\alpha = 0$.

A percolation measurement began with a coloring of the lattice with random numbers, produced by a Fibonacci generator. All clusters on the lattice were then constructed (between adjacent sites with random numbers valued less than p) using the method of Hoshen and Kopelman[33]. For smaller lattices and smaller values of the central charge, percolation clusters were built after each update of the lattice and matter. For $c \geq 1$ we found that it was more efficient to construct clusters after every 5-10 updates of the lattice. For $c < 1$, clusters were formed using several different values of p for each lattice. For smaller lattices, the values of these observables could be extrapolated to nearby values of p using histogramming techniques [34]. Thus, for $c < 1$, there are strong correlations between the values of observables at different values of p. Histogramming proved to be less reliable for larger lattices and for $c \geq 1$. For $c \geq 1$, our statistics were not quite so good and we were thus more wary of statistical artifacts influencing our interpretation of the data. We therefore performed entirely independent simulations for each value of p, so data points at different p would be uncorrelated.

Our errors were computed using the jackknife technique. We first used the jackknife error to estimate the auto-correlation time, $\tau \sim 1/2(\sigma_{jack}/\sigma_{naive})^2$; σ_{naive} is just the standard error, assuming no correlations. Additionally, we measured the auto-correlation function, and using standard methods [35] and appropriate fits, determined the integrated autocorrelation times (with errors on these times obtained via jacknife). Generally, these two techniques yielded

consistent results. For some of the largest lattices, the fits to the auto-correlation function were more reliable, since the jackknife error did not plateau convincingly as a function of increasing bin-size. Thus, some of the estimates of the error bars for data on the largest lattice ($N = 16384$) might be a bit off.

To obtain the desired precision for our observables, we sampled a large number of lattices – between 3×10^4 and 2.5×10^5 independent samples, requiring up to 2×10^6 sweeps per data point. We performed the simulations on HP 9000, IBM RS6000 and DEC MIPS workstations; in total we used roughly the equivalent of 5 months of time on a HP workstation to gather our data. Our lattices were of toroidal topology. For $c = 0$, we used lattices of size 512 through 16384; for $c = 1/2$ our lattices ranged in size from $N = 2048$ to 16384. The correlation times were much longer for $c = 1$ and 2; thus the $c = 1$ runs were performed for $N = 1024$ through 8192 at $p_c = 1/2$ and 1024 and 2048 for other p. $c = 2$ runs were only done on lattices of size 1024 and 2048 and also at $p = 1/2$ using $N = 4096$.

Our basic set of observables consisted of : the number of clusters per unit volume $K(p)$, the maximum cluster size per configuration $\mathcal{M}(p)$ and the mean cluster size $\mathcal{S}(p)$.

Our other main task was to determine the critical temperature, to verify that $p_c = 1/2$ for $c \leq 1$ and then to look for p_c for $c > 1$. Finding an appropriate technique to do this was not so straightforward. To illustrate this difficulty, we first recall that the width of the transition region is of magnitude $N^{1/\nu d_H}$. This width should be, for instance, roughly comparable to the breadth of the susceptibility peak (the mean cluster size with the infinite, i.e. largest, cluster excluded) and its asymptotic shift from $p_c(N = \infty)$. For $c \leq 1$, νd_H ranges from 4 to about 4.7, indicating that the transition will be extremely broad; for lattices of several thousand nodes, $\delta p \sim .1$ to $.2$. In contrast, $\nu d = 2$ for the $2d$ (flat space) Ising model, which will exhibit a transition that is an order of magnitude sharper on lattices of comparable size.

In fact, significant effort has been devoted to developing methods to determine percolation thresholds precisely. Unfortunately, nearly all of the standard techniques are inapplicable in our case. They involve determining the fraction of spanning clusters (see e.g. [36]) or comparing the outside and inside perimeters of clusters [37]. These methods rely on the identification of a lattice boundary, which we cannot do easily on random lattices. Other techniques also exploit exact analytic results for small cluster sizes [38], which are not available to us in this case. We therefore ended up adopting a variant of a standard technique used in spin models, which relies on a determination of intersections of Binder's cumulants.

Explicitly, we shall consider the quantities

$$u_S = 1 - \frac{\langle S^2 \rangle}{3(\langle S \rangle)^2}$$ (26)

and

$$u_{\mathcal{M}} = 1 - \frac{\langle \mathcal{M}^2 \rangle}{3(\langle \mathcal{M} \rangle)^2}.$$ (27)

These quantities should obey (for $c < 1$ at least) a finite-size scaling form

$$u_{S,\mathcal{M}}(N, p) \asymp f_{S,\mathcal{M}}(z); \quad z = (p - p_c) N^{1/\nu d_H}.$$ (28)

f is the universal finite-size scaling function and z is the appropriate scaling variable. The deviation of these cumulants from 2/3 just characterizes the magnitude of fluctuations of the mean and maximum sizes. For $p \to \infty$, $f \to 2/3$, since in this phase, the infinite cluster saturates the system and fluctuations diminish. Asymptotically, the cumulants for different values of N will intersect at $p = p_c$ (which is much better than $p \sim p_c \pm N^{1/\nu d_H}$) where they will be linear and have slope $f'(0) N^{1/\nu d_H}$. Therefore, the slopes will not be particularly large, and they will grow slowly; determining the points of intersection will require very good statistics.

We briefly digress to point out how the cumulant u_S is related to the standard Binder's cumulant in spin models, $u = 1 - \langle M^4 \rangle / 3 (\langle M^2 \rangle)^2$; M is the magnetization. Although it is true that $\langle S \rangle = \langle M^2 \rangle$, in general $u \neq u_S$. In the Ising model (and this should presumably generalize to all q-state Potts models), one can easily derive the relation:

$$\langle M^4 \rangle = 3 \langle S^2 \rangle - \frac{2}{N} \langle \int n(s) s^4 / \int n(s) s \rangle;$$ (29)

$n(s)$ is again the cluster distribution function and the latter term is proportional to the probability that 4 black points in the lattice lie together in the same cluster. The sum of the terms, which both scale the same way in N, is thus just the integrated 4-point function of the spin-operator, with a value that should in principle be calculable analytically. So our cumulant just measures one (non-negligible) piece of this 4-point function.

5 Numerical Results

5.1 Correlation Times

We now turn to the results of our simulations. First, we remark that we observed considerable critical slowing down for $\mathcal{M}(p)$ and $S(p)$ for all values of c. We

Table 1: A summary of the critical slowing down exponent z/d_H for our runs

	$c = 0$	$c = 1/2$	$c = 1$	$c = 2$
$z_{\mathcal{M}}/d_H$	.69 (2)	.75 (6)	1.5 (2)	1.4 (2)
z_S/d_H	.70 (2)	.74 (6)	1.4 (2)	1.4 (2)

found that the values of the auto-correlation exponent z/d_H : $\tau \sim N^{z/d_H}$ were identical, within our statistics, for S and $\mathcal{M}$. In the following table we summarize the values of these exponents.

For $c = 0$, the dynamics consists solely of the *local* link flip updates. Since our cluster observables exhibit considerable slowing down, they reflect large-scale correlations in the geometry of the worldsheet. In contrast, measurements of the distribution of curvature (e.g. of $\sum_i |q_i - 6|$) do not exhibit measurable critical slowing down. d_H has been estimated to be about 2.87 for $c = 0$ [40, 3]; this leads to a value of z of 2.0. The value $z/d_H \sim .7$ is not the largest value that one might anticipate. For, one would naively guess that the decorrelation of the slowest critical modes of the surface geometry would be determined by the spectral dimension, $d_s = 2$ [3], which characterizes the probability that a random walker returns to its original site after time t, $P(t) \sim t^{-d_s/2}$. Thus effectively a random update would take a time proportional to N (corresponding to $z/d_H = 1$) to diffuse across the surface.

Critical slowing down becomes more severe with increasing c. This could be partially due to changes in the fractal properties of the geometry; presumably the updates of the matter induce additional slowing down also. Since the change in z/d_H from $c = 0$ to $c = 1/2$ is rather small, it appears that the Swendsen-Wang algorithm is quite efficient for our measurements. Further discussion of the efficiency of spin algorithms on random lattices will appear in [41]. Our auto-correlation times range from about $\tau_{int} = 1$ (for $c = 0, N = 512$) to 50 (for $c = 2, N = 2048$). Although z/d_H is virtually identical for $c = 1$ and $c = 2$, the correlation times for $c = 2$ are consistently about a factor of 3 higher than the corresponding $c = 1$ times. Probably, cluster methods would have been more efficient in updating the Gaussian fields [42].

We observed one other curious difference between auto-correlation functions for $c = 0$ and $c > 1$. For $c = 0$, the fits of the auto-correlation function (as a function of time T) to the form $\exp(-T/\tau)$ were excellent for $T > 3\tau$ and all values of N. For $c > 1$, this was no longer true. The auto-correlation functions for $c = 2$ were quite difficult to fit to; even for times considerably larger than τ, they exhibited very strong transients. We shall argue in subsequent sections

that for $c > 1$ that we do not observe good scaling behavior; the behavior of the auto-correlation functions could perhaps be interpreted as a first hint that this might be so.

5.2 Critical Exponents and KPZ

We now present tables of the effective critical exponents $(d_f/d_H)_{eff} \equiv \ln(\mathcal{M}_{2N}/\mathcal{M}_N)/\ln 2$ followed by $(\gamma/\nu d_H)_{eff} \equiv \ln(\mathcal{S}_{2N}/\mathcal{S}_N)/\ln 2$ obtained through finite-size scaling at $p = 1/2$, as defined in section 4.

The exact values for $\gamma/\nu d_H$, obtained from (7) and (11) are 3/4, $(4 - \sqrt{7/2})/3$ and $1 - \sqrt{5/24}$ for $c = 0$, $1/2$ and 1 respectively. We have again used $d_f/d_H = \frac{1}{2}(1 + \gamma/\nu d_H)$. First, we remark that the agreement between the theoretical values and our measurements for $c < 1$ is surprisingly good, given that our runs are on medium-sized lattices. The exponents generally decrease as a function of increasing lattice size and central charge c. This seems reasonable, since embryonic universes with necks of the size of the cutoff become more dominant as c increases; we can see from the theoretical calculations that this corresponds to a reduction in the critical exponents. For N not so much larger than the cutoff, the effect of these bottlenecks should be not so apparent and then presumably the critical exponents would be over-estimated. For $c = 0$ on the larger lattices, the exponents have more or less already leveled off, within our statistics, to their asymptotic values.

For $c = 1$, if we simply assumed that $\mathcal{S}$ and $\mathcal{M}$ scaled as powers of N, then our estimates of the critical exponents will be very far off. In fact, the measured values of the effective $c = 1$ exponents agree quite well with the theoretical predictions for $c = 1/2$. The logarithmic corrections, though, will shift the effective exponents far away from their asymptotic values. Using the relations

	c = 0	c = 1/2	c = 1	c = 2
N = 512	.879 (2)		.860 (5)	
N = 1024	.880 (3)		.861 (5)	.81 (1)
N = 2048	.880 (3)		.859 (7)	.83 (2)
N = 4096	.871 (4)	.866 (6)	.841 (8)	
N = 8192	.875 (5)	.852 (8)		
theory	.875	.855	.772	

Table 2: Measurements of $(d_f/d_H)_{eff}$ compared with theoretical predictions of the $N \to \infty$ limit

(16) and (17) we see that the first subleading contribution yields

	c = 0	c = 1/2	c = 1	c = 2
N = 512	.774 (2)		.744 (6)	.68 (2)
N = 1024	.772 (4)		.739 (7)	.67 (3)
N = 2048	.768 (5)		.747 (6)	.732 (7)
N = 4096	.753 (5)	.741 (7)		
N = 8192	.755 (7)	.722 (10)	.700 (10)	
theory	.75	.710	.544	

Table 3: Measurements of $(\gamma/\nu d_H)_{eff}$ compared with theoretical predictions of the $N \to \infty$ limit

$$(\gamma/\nu d_H)_{eff} = \gamma/\nu d_H + \frac{1 + \gamma/\nu d_H}{\ln N} + \cdots. \qquad (30)$$

In the following plot, we compare our data for $(\gamma/\nu d_H)_{eff}$ at $c = 1$ with the theoretical prediction, derived from (16) and (17). We plot (30) with the dotted curve. The solid curve takes into account all corrections in (16) and (17); the smallest correction in the expansion we used to generate this theoretical prediction was of order .002 for $N > 1000$. At this order further corrections arising from the logarithmic renormalization of μ, which we did not compute or conjecture to be universal, should appear. We therefore would guess (without any rigorous justification) that these additional corrections should probably shift the curve by less than the statistical accuracy of our data, which is roughly .01. For $c < 1$ we observed small systematic discrepancies from asymptotic scaling, presumably from power law corrections. Since power law corrections have also not been taken into account at $c = 1$, we consider the agreement between our measurements and the both $c = 1$ theoretical curves is thus quite good, certainly comparable to the agreement for $c < 1$. This suggests the likelihood that at least the leading $c = 1$ logarithmic correction to scaling (30) is indeed universal. We emphasize that we cannot predict the presence of logarithms in the finite-size scaling ansatz from our data, since it is not nearly precise enough to distinguish logarithmic behavior from a small power law. We can clearly see, though, that if we assume the logarithmic scaling ansatz given in (16) and (17), that we can extract the proper value of $\gamma/\nu d_H$ from our data within an accuracy of a few percent. Also, the agreement between our data and the KPZ prediction is quite sensitive to the power with which the leading logs appear in the finite-size scaling ansatz.

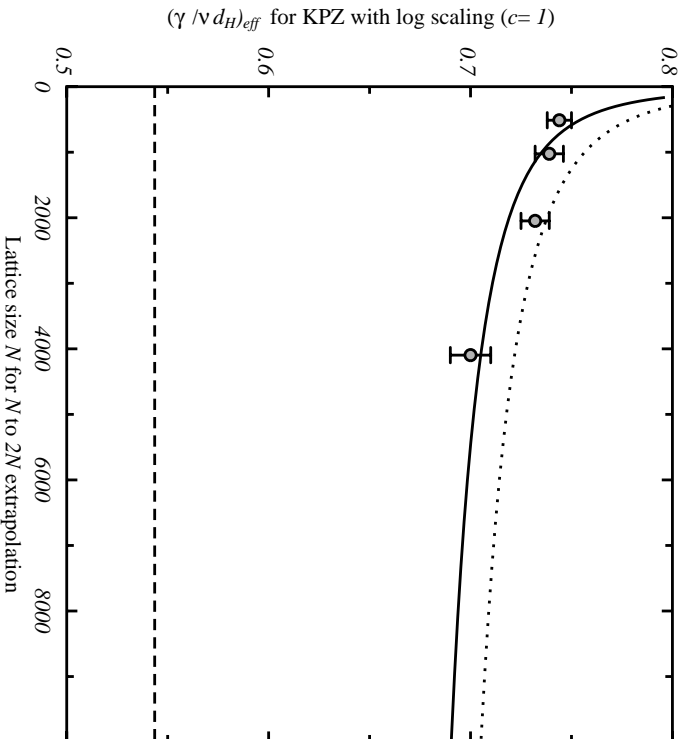Naively, it appears that since the effective exponents for $c = 1/2$ and $c = 1$

Figure 3: A comparison of the theoretical prediction of the finite size $c = 1$ scaling of $\gamma/\nu d_H$ with our data. The dotted line includes the leading logarithmic correction and the solid line takes into account all subleading terms that we calculated. The horizontal dashed line indicates where these curves asymptote.

that we measured are quite similar, that the coupling to matter in both theories also is qualitatively of the same magnitude. We see now that this should not be true in the continuum limit where the exponents are really very different. One would need to simulate the $c = 1$ model on a 400000 node lattice to see $(\gamma/\nu d_H)_{eff}$ decrease to .65, which would be a somewhat appreciable, though not tremendous difference from the $c = 1/2$ value of .71; $(\gamma/\nu d_H)_{eff} \sim .60$ for 10^{12} triangles. One might think that there is a bit of a conspiracy occurring here: the $c = 1$ KPZ exponents and the logarithmic finite scaling ansatz somehow mysteriously combine to produce behavior that strongly resembles $c \sim 1/2$ on lattices that are numerically accessible to us. The discussion in section (6) should demystify this observation, though.

5.3 Determining p_c

We now ascertain if we can successfully estimate p_c from our data. First, we verify numerically the identity (24), which constrains p_c to be 0, 1/2 or 1 for non-integer α. In figure 4 we have plotted $K(1 - p) - K(p)$ (recall that K equals the number of clusters per site) versus $2p(p-1/2)(1-p)$ using data from $c = 0$ simulations with $N = 8192$. Note that all data points in this plot are heavily correlated; we used histogramming (from samples taken at $p = .49, .50$ and .51) to produce all of the data points. Clearly the agreement is excellent, as expected, since (24) should be correct up to corrections of order $1/N$ for genus 1.

Next, we examine the intersection of the cumulants $u_M(p)$ and $u_S(p)$ for $c = 0$, presented in figures 5 and 6 for lattice sizes $N = 1024, 2048$ and 4096. The curves intersect around $p_c = .506(4)$ and .508(4) respectively, within a percent or two of the exact value of $p_c = .5$. Considering that the large value of νd_H implies that the width of the transition is of order .15, we conclude that this technique is fairly successful in locating the critical point in this case. For $c = 1/2$, this technique is at least moderately successful; the intersection point occurs roughly around .51. We demonstrate this in figure 7, which shows the curves u_M for $N = 2048, 4096$ and 8192.

At $c = 1$, the intersection point of u_S, as shown in figure 8, has moved quite a bit to the right. Its position is difficult to determine given our statistics, but it appears to be above $p = .52$ and below .56. The data points in this plot are each statistically independent; we have foregone histogramming because it is no longer so reliable. Since we know that $p_c = .5$ from equation (24) in this case, we can see that the method of intersections now has become much less reliable. This failure is expected, though, since the cumulants will only intersect near p_c when one has reached the scaling regime where (28) is valid. One would expect
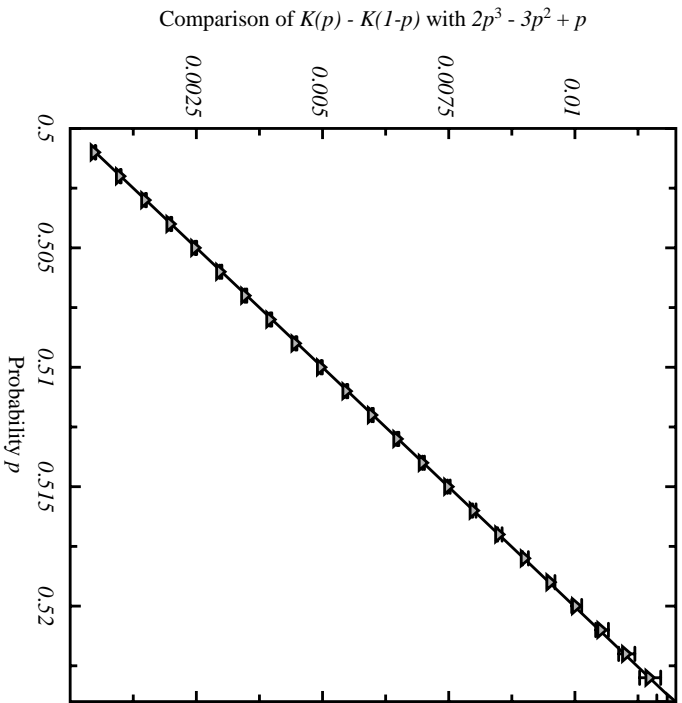
Comparison of *K(p) - K(1-p)* with $2p^3 - 3p^2 + p$

Figure 4: A comparison of the theoretical prediction relating the the number of clusters per unit area to a polynomial in p. The data is from $c = 0$ simulations on lattices of size 8192.
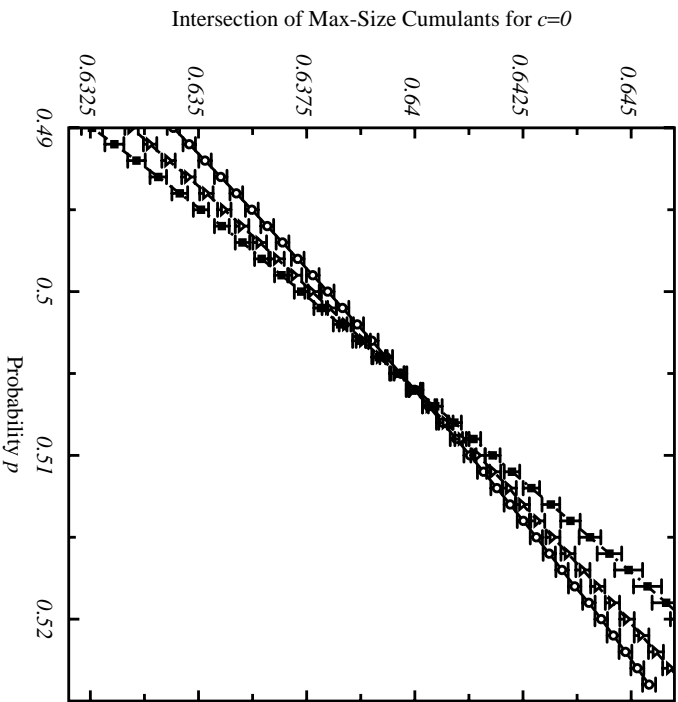
Intersection of Max-Size Cumulants for *c=0*

Figure 5: The cumulants $u_M(p)$ for gravity with no matter. The circles refer to lattice size $N = 1024$, $N = 2048$ points are labeled by triangles, and the squares correspond to $N = 4096$.
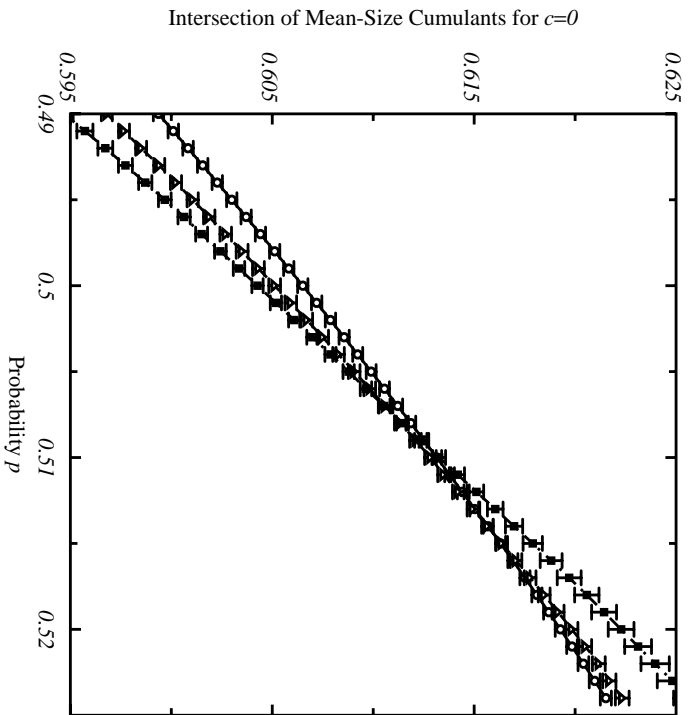
Intersection of Mean-Size Cumulants for *c=0*

Probability *p*

Figure 6: The cumulants $u_S(p)$ for gravity with no matter. Points are labeled as in the preceding figure.

Intersection of Max-Size Cumulants for *c=1/2*

Probability *p*

Figure 7: The cumulants $u_M(p)$ for gravity coupled to $c = 1/2$ matter. Again, $N = 2048$ points are labeled by triangles, $N = 4096$ data is represented by squares; the circles correspond to $N = 8192$.
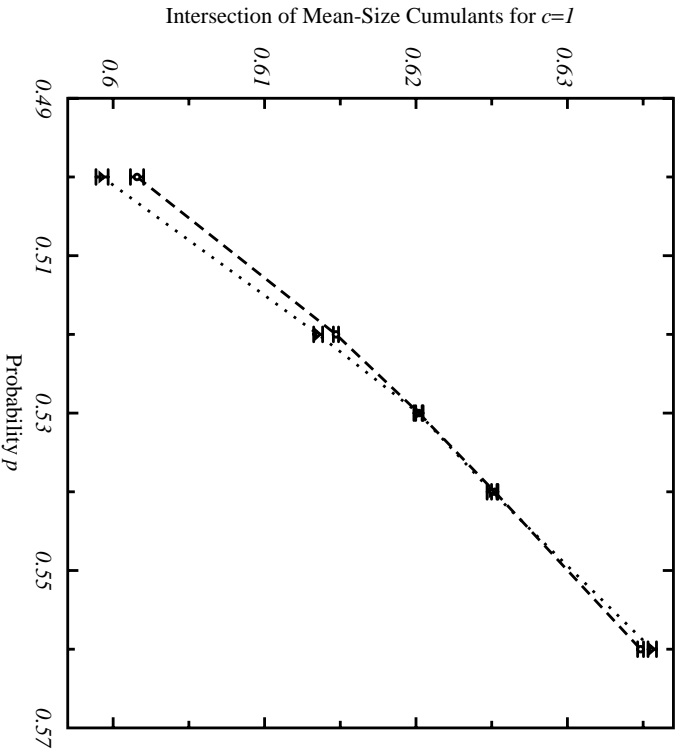
that the log corrections to scaling would modify (28) to a relation roughly like

$$u_{S,\mathcal{M}}(N,p) \asymp (1 + \frac{C}{\ln N}) f_{S,\mathcal{M}}(z),$$ (31)

(the definition of the scaling variable z should also receive logarithmic corrections). This modification is anticipated because continuum observables (such as $f(0)$) seem to generically receive $1/\ln N$ corrections at $c = 1$. Note that as c increases and bottlenecks on the worldsheet become more prominent, the values of the cumulants (at $p = .5$) decrease, indicating that our observables experience greater fluctuations. Similarly, increasing N will make the presence of necks more apparent; this should lead to a decrease in a cumulant, implying that the constant C in (31) is positive. This will then result in a shift in the intersections to larger values of p, as observed.

For $c = 2$, the intersection moves even further to the right. We illustrate this in figure 9; all points in this figure are again statistically independent. In fact, we cannot determine whether the cumulants actually intersect or just asymptotically merge, since they have not even crossed over each other within our statistics at $p = .65$. Clearly, though, there is no intersection between $p = .50$ and $p = .56$. At first glance, this appears to be exactly what we were looking for. Our original goal was to determine if p_c was appreciable far from .5. If this were true in the continuum, one would infer that either a transition was absent for $p < 1$ or that perhaps the worldsheet admitted a mean-field percolation transition; either scenario would be more characteristic of percolation on trees. One might hope that the merging of cumulants closer to .6 as observed would just indicate that the percolation correlation length had finally grown to well beyond the size of our lattices.

The above scenario, however, is somewhat implausible. Note that the effective exponents, e.g. $\gamma/\nu d_H$ do not change dramatically at $p = .5$ from $c = 1$ and $c = 2$. In general, the $c = 2$ and $c = 1$ surfaces do not appear qualitatively so different, so one might doubt that the percolation correlation length, which is infinite at $p = .5$ and $c = 1$ has decreased to roughly the lattice size or below for $c = 2$. We saw that the intersection of the cumulants was shifted because of finite-size effects at $c = 1$. Presumably finite-size effects could also play a large role at $c = 2$, so perhaps the large (at least 15% of p!) shift we see in the cumulants is just a finite lattice artifact. We shall argue in the following section that this is indeed probably true and that in fact any measurements for c somewhat greater than 1 will primarily be manifestations of lattice artifacts. Let us remark that at least we have observed, via these cumulants, that the behavior of $c < 1$ and $c = 2$ is qualitatively different. The presence of non-analytic behavior of $K(p)$ at $p = p_c$ along with good scaling behavior on the lattices we consider mandates that the cumulants intersect near $p = 1/2$, as observed for $c < 1$. This

Intersection of Mean-Size Cumulants for *c=1*

Figure 8: The cumulants $u_S(p)$ for gravity coupled to a Gaussian field. The circles and dashed lines represent $N = 1024$ data and $N = 2048$ points are labeled by triangles connected by dotted lines. Lines are drawn to guide the eye.

Intersection of Mean-Size Cumulants for c=2

Probability p

Figure 9: The cumulants $u_s(p)$ for gravity coupled to two Gaussian fields. Points and lines are labeled as in the preceding figure.

---

clearly is not the case for $c = 2$.

6   Discussion

To understand what we are seeing at $c = 2$, we return to a discussion of the scaling corrections for $c = 1$. A simple physical description of the origin of these corrections can be found in Klebanov's review [16]. We begin by considering the $c = 1$ tachyonic operator of momentum p:

$$T(p) \sim \int \sqrt{|\hat{g}|} \, \overline{\exp}(ipX + (|p| - 2)\phi); \tag{32}$$

ϕ is the Liouville field and $\hat{g}$ is the reference metric ($g = \hat{g} \exp(-\phi)$). The Gaussian field obeys [43]

$$\langle XX \rangle \sim (\ln N)^2. \tag{33}$$

Thus, the finite lattice size effectively imposes an infrared cutoff on spacetime momenta of order $1/\ln N$. The tachyonic energy satisfies

$$E^2 = p^2 + \frac{1-c}{12}. \tag{34}$$

Therefore, the minimum ground state energy accessible at $c = 1$ on a lattice of size N should be roughly

$$E_{min}^2 \sim \left(\frac{C}{\ln N}\right)^2, \tag{35}$$

for some constant of order unity C. This correction can be quite large; it contributes to the logarithmic dressing of correlation functions and thus the logarithmic corrections we have measured that mask the degeneration of the worldsheet.

Furthermore, one would anticipate that for finite N, the Gaussian model coupled to gravity should qualitatively resemble a range of $c < 1$ models. For the $c < 1$ conformal field theories can be expressed as continuum limits of lattice models in which the worldsheet is embedded on Dynkin diagrams [44]. $c = 0$ corresponds to an embedding into $\mathcal{A}_2$, $c = 1/2$ to $\mathcal{A}_3$ and $c \to 1$ is identified with the $n \to \infty$ limit of $\mathcal{A}_n$. For fairly large n, the finite worldsheet lattice size imposes an effective cutoff on these diagrams and screens out the presence of all but a few Dynkin vertices, producing behavior characteristic of lower c.

The same mechanism should be in force for $c > 1$. The extrinsic Hausdorff dimension, D_H, may no longer be infinite but it presumably is large. If branched polymers do dominate in the large c limit, then $D_H(c = 1) = \infty$ and $D_H(c \gg$
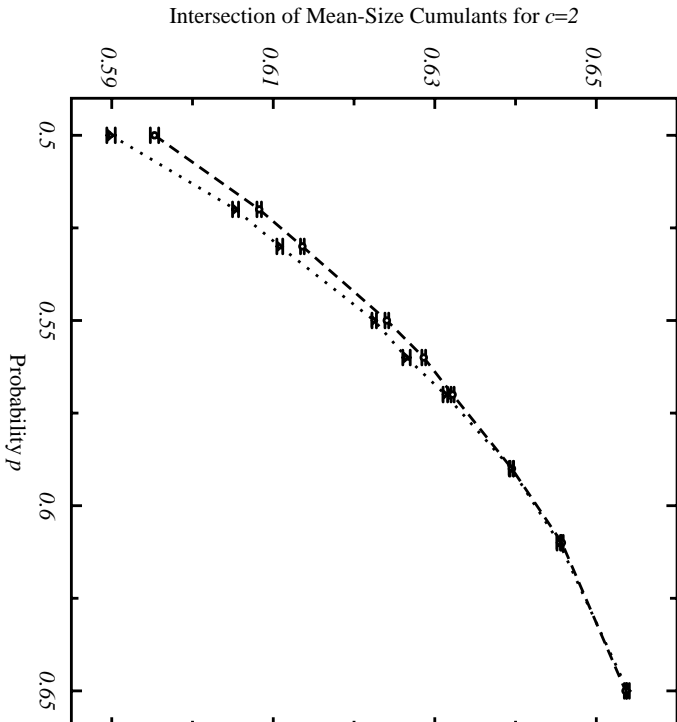
1) $= 4$ [2, 26] [9]. Numerical work has indicated that for c of about 2 or 3, that D_H is roughly $8 - 10$ [45, 46], though these values are probably not reliable in [10]. For $c > 1$, one would then expect that the minimum ground state energy accessible on a lattice of size N would be roughly

$$E_{min}^2 \sim (\frac{C}{N^{1/D_H}(N,c)})^2 + \frac{1-c}{12}, \qquad (36)$$

where again C is a constant of order unity, perhaps with a factor of 2π thrown in. For fixed N, one would only expect to observe a gradual increase in the density of bottlenecks that pinch off large baby universes as c increases and E_{min} effectively decreases. A degeneration of the worldsheet into a polymer-like structure would only become clearly apparent when c reaches a value such that (36) is approximately zero. Numerically, it has been observed that this degeneration is evident roughly when c is about 10-12 for lattices of order $N = 10^3$. If we assume that at this point $D_H = 4$ [46], then this determines the constant C to be about $6 \sim 2\pi$, an entirely reasonable value. Of course, these should be only interpreted as back of the envelope estimates, designed to show that this scenario is qualitatively consistent with numerical observations.

At $c = 2$, E_{min} reaches 0 when $N \sim C^{D_H(c=2)} 12^{D_H(c=2)/2}$. Thus, if either C is somewhat greater than 1 (e.g. 6 as in the previous paragraph) or if $D_H(c = 2)$ is rather large, one would need extraordinarily large lattices to directly see the degeneration of the worldsheet. For instance, $C = 6$ and $D_H(c = 2) = 10$ yield $N \sim 2.5 \times 10^5$. If C is not larger than 1 and $D_H(c = 2)$ is smaller (near 4, for example) then the tachyonic degeneration should be observable on the lattices we consider and finite-size effects should not be so dominant. These values, however, would then not be consistent with previous much larger measurements of $D_H(c = 2)$. Again, we do not advocate taking particular numbers too seriously. It is apparent, though, that the true continuum behavior at $c = 2$ might only become evident at scales orders of magnitude larger than those that are amenable to simulation.

One would then expect also that the percolation correlation length at $p = .5$ (where a transition would occur for surfaces) should be comparable to the length scale at which the surface degenerates into a branched polymer. If we accept the possibility that this length scale is very large, then for $c = 2$, we should not be able to detect the presence of this correlation length on surfaces of a few thousand nodes. From the relation (36) it follows that we should observe significant deviations from scaling, since the shift in the effective ground state mass

is detectable as a function of N (as at $c = 1$). In fact, $1/\ln(10^3) < 1/(10^3/D)$ for $D > 4$, so for the range of N that we simulate, the shifts in finite-size corrections could be larger for $c = 2$ than for $c = 1$. Therefore, the large shift in the cumulant intersections at $c = 2$ is most likely just a manifestation of a lack of good scaling behavior. All other possibilities do not fit very well with at least some portion of the prevailing numerical evidence. If at $c = 2$ the worldsheet had degenerated into a tree-like structure, and our measurements were indeed satisfactorily measuring asymptotic scaling behavior, then some evidence of the tachyonic degeneration should have been easily apparent in previous simulations. If on the other hand, no such surface degeneration had occurred and our measurements were within the scaling regime, then we would have not anticipated a large shift in the cumulant intersection from $p = .5$.

This leads us to a rather disappointing conclusion. The above arguments suggest the likelihood that generically numerical simulations for c somewhat greater than one will just measure lattice artifacts. This has also been borne out by previous attempts to measure γs, which indicated that corrections to scaling were predominant for $c \geq 1$ [25]. On lattices of accessible size, the onset of the tachyon could be hidden by finite-size effects, and we would fail even to capture the qualitative nature of these models in the continuum limit. Scaling exponents and critical properties of the geometry (the Hausdorff dimension, e.g.) measured in these simulations would not describe continuum scaling behavior. For very large c, simulations may reflect the character of the tachyonic instability, however. At $c = 1$, the results of simulations can only be properly understood if one knows the form of the corrections to scaling, which can be computed because the theory is solvable. For $c < 1$, we have found that numerical simulations do reproduce, with reasonable precision, critical exponents that characterize the behavior of percolation on strings.

7 Acknowledgments

References

[1] J. Distler, Z. Hlousek and H. Kawai, Int. J. Mod. Phys **A5** (1990) 1093.

[2] F. David, Nucl. Phys. **B368** (1992) 671.

[3] M.E. Agishtein, R. BenAv, A. Migdal and S. Solomon, Mod. Phys. Lett. **A6** (1991) 1115.

[4] H. Kawai, N. Kawamoto, T. Mogami and Y. Watabiki, Phys. Lett. **B306** (1993) 19.

[5] S. Jain and S. Mathur, Phys. Lett. **B286** (1992) 239.

[6] J. Ambjørn, S. Jain and G. Thorleifsson, Phys. Lett **B307** (1993) 34.

[7] N. Seiberg, Prog. Theor. Phys. Suppl. **102** (1990) 319.

[8] G. Moore and P. Ginsparg, " Lectures on 2-D Gravity and 2-D String Theory ", TASI Lectures, Yale preprint YCTP-P23-92 and Los Alamos preprint LA-UR-92-3479 (1993), hep-th/9304011.

[9] M.E. Cates, Europhys. Lett. **7** (1988) 719.

[10] E. Brézin and S. Hikami, Phys. Lett. **B283** (1992) 203; S. Hikami and E. Brézin, Phys. Lett. **B295** (1992) 209; S. Hikami, Phys. Lett. **B305** (1993) 327.

[11] M. Wexler, Phys. Lett **B315** (1993) 67.

[12] J. Ambjørn, B. Durhuus, T. Jónsson and G. Thorleifsson, Nucl. Phys. **B398** (1993) 568.

[13] S. M. Catterall, J. B. Kogut and R. L. Renken, Phys. Rev. **D45** (1992) 2957; Phys. Lett. **B292** (1992) 277.

[14] C. Baillie and D. Johnston, Mod. Phys. Lett. **A7** (1992) 1519; Phys. Lett. **B286** (1992) 44.

[15] F. David, "Simplicial Quantum Gravity and Random Lattices", Saclay preprint T93-028, to appear in Les Houches proceedings on " Gravitation and Quantizations ".

[16] I. Klebanov, *String Theory in Two-Dimensions*, in Proc. of the Trieste School on "String Theory and Quantum Gravity '91" (hep-th/9108019).

[17] M. Bowick, M. Falcioni, G. Harris and E. Marinari, " Two Ising Models Coupled to 2–Dimensional Gravity ", Syracuse University preprint 4241-556.

[18] V. G. Knizhnik, A. M. Polyakov and A. B. Zamolodchikov, Mod. Phys. Lett. **A3** (1988) 819.

[19] J. W. Essam and M. E. Fisher, J. Math. Phys. **2** (1961) 609.

[20] V. A. Kazakov, Mod. Phys. Lett. **A4** (1989) 1691.

[21] M. den Nijs, Phys. Rev. **B27** (1983) 1674.

[22] F. David, Mod. Phys. Lett. **A3** (1988) 1651; J. Distler and H. Kawai, Nucl. Phys. **B321** (1989) 509.

[23] G. Parisi, Phys. Lett. **B238** (1990) 209; D. J. Gross and N. Miljkovic, Phys. Lett **B238** (1990) 217; E. Brézin, V. Kazakov and Al. B. Zamolodchikov, Nucl. Phys. **B338** (1990) 673; P. Ginsparg and J. Zinn-Justin, Phys. Lett. **B240** (1990) 333; D. J. Gross and I. R. Klebanov, Nucl. Phys. **B344** (1990) 475.

[24] D. Stauffer and A. Aharony, *Introduction to Percolation Theory* (Taylor and Francis, London, U.K. 1992).

[25] J. Ambjørn, D. Boulatov and V. A. Kazakov, Mod. Phys. Lett. **A5** (1990) 771.

[26] J. Ambjørn, B. Durhuus, J. Fröhlich and P. Orland, Nucl. Phys. **B270** (1986) 457; J. Ambjørn, B. Durhuus and J. Fröhlich, Nucl. Phys. **B275** (1986) 161.

[27] M. F. Sykes and J. W. Essam, J. Math. Phys. **5** (1964) 1117.

[28] J. van den Berg, J. Math. Phys. **22** (1981) 152.

[29] D. Boulatov, V. Kazakov, I. Kostov and A. A. Migdal, Phys. Lett. **B157** (1985) 295.

[30] R.H. Swendsen and J.-S. Wang, Phys. Rev. Lett. **58** (1987) 86.

[31] Z. Burda and J. Jurkiewicz, Acta Physica Polonica **B20** (1989) 949.

[32] J. Jurkiewicz, A. Krzywicki, B. Petersson and B. Söderberg, Phys. Lett. **B213** (1988) 511.

[33] J. Hoshen and R. Kopelman, Phys. Rev. **B14** (1976) 3428.

[34] M. Falcioni, E. Marinari, M. L. Paciello, G. Parisi and B. Taglienti, Phys. Lett. **102B** (1981) 270; A. M. Ferrenberg and R. H. Swendsen, Phys. Rev. Lett. **61** (1988) 2635; and *Erratum*, ibidem **63** (1989) 1658.

[35] A. Sokal, " Monte Carlo Methods in Statistical Mechanics: Foundations and Algorithms ", NYU preprint based on lectures at the Troisième Cycle de la Physique en Suisse Romande, June 1989.

[36] S. Kirkpatrick, in "Ill–Condensed Matter", Les Houches Proceedings, Vol.31, ed. R. Balian, R. Maynard and G. Toulouse (North Holland, Amsterdam 1983) 372.

[37] R. Ziff, Phys. Rev. Lett. **56** (1986) 545; M. Rosso, J. F. Gouyet and B. Sapoval, Phys. Rev. **B32** (1985) 6053.

[38] Z. Djordjevic, H. E. Stanley and A. Margolina, J. Phys. **A15** (1982) L405.

[39] K. Binder, Z. Phys. **B43** (1981) 119.

[40] H. Kawai and M. Ninomiya, Nucl. Phys. **B336** (1990) 115.

[41] M. Bowick, M. Falcioni, G. Harris and E. Marinari, to appear.

[42] T. Filk, M. Marcu and B. Scheffold, Proceedings of Lattice 92, Amsterdam (North Holland, Amsterdam 1993) 783

[43] V. A. Kazakov and A. A. Migdal, Nucl. Phys. **B311** (1988) 171.

[44] V. Pasquier, J. Phys. **A20** (1987) 5707.

[45] A. Billoire and F. David, Nucl. Phys. **B275** (1986) 617; D. Boulatov, V. Kazakov, I. Kostov and A. A. Migdal, Nucl. Phys. **B275** (1986) 641.

[46] J. Jurkiewicz, A. Krzywicki and B. Petersson, Phys. Lett. **B168** (1986) 273.